Performance of alumina-forming duplex stainless steels (ADSS) as accident tolerant fuel cladding materials

Changheui Jang[1*],
Hyunmyung Kim[1,3], Chaewon Kim[1],
Kangsan Kim[1], Yonghee Kim[1], Seungjae Lee[2], Hun Jang[2]

장창희, 김현명, 김채원
김강산, 김용희
이승재, 장훈

Wed. Oct. 23rd, 2019

[1]Korea Advanced Institute of Science and Technology (KAIST)
[2]KEPCO Nuclear Fuel (KNF)
[3]Korea Institute of Industrial Technology (KITECH)

Contents

- **Background**
- **Development of alumina-forming duplex SS**
  - Microstructure
  - Tensile properties
  - Corrosion resistance
  - Thermal aging embrittlement
- **Neutronics Aspects of ADSS Alloys**
  - Neutron penalty on fuel cycle
  - Helium production
  - Decay heat
- **Fabrication of thin cladding tubes**
- **Summary**

Background

Background

S. Zinkle et. al., J. Nucl. Mater., 448 (2014) 347

❑ Accident Tolerant Fuel (ATF) Cladding

- Fukushima Daiichi (Japan) nuclear power station accident in March 2011 from tsunami and hydrogen explosion

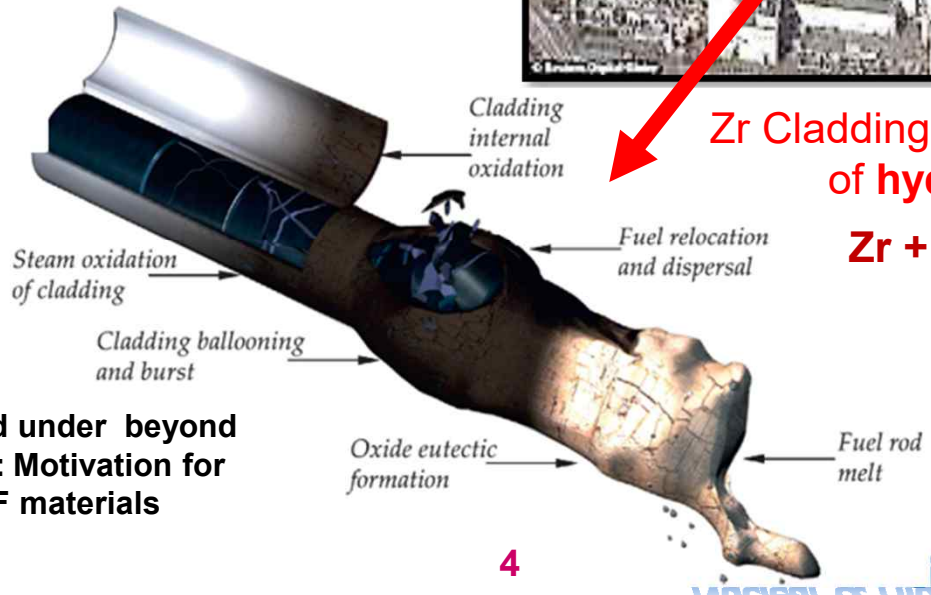

Zr Cladding oxidation: **Major source** of **hydrogen** generation

$$Zr + 2H_2O \rightarrow ZrO_2 + 2H_2 + \Delta H$$

▶ **Evolution of a fuel rod under beyond design-basis accidents: Motivation for development of ATF materials**

Background

[1] B. Pint ORNL report Pub58127, 2015
[2] Y. Yamamoto ORNL report Pub58715, 2015
[3] B. Cheng EPRI 2015 technical report 3002005557, 2015

❑ Candidate ATF cladding materials

- **FeCrAl:** Fe-base alloys, Optimized for key performance + tube fabrication
- **Coated Zr:** Near-term industrial (AREVA, Westinghouse) implementation
- **Domestic (Korean):** Cr/Al-coated (KAERI) Zr-alloys

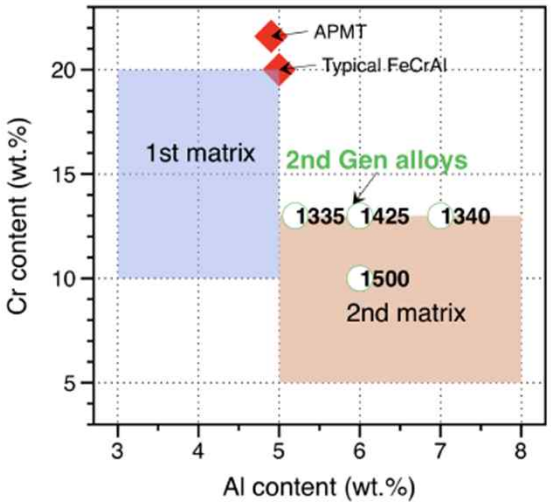

▲ FeCrAl alloys target compositions [1]

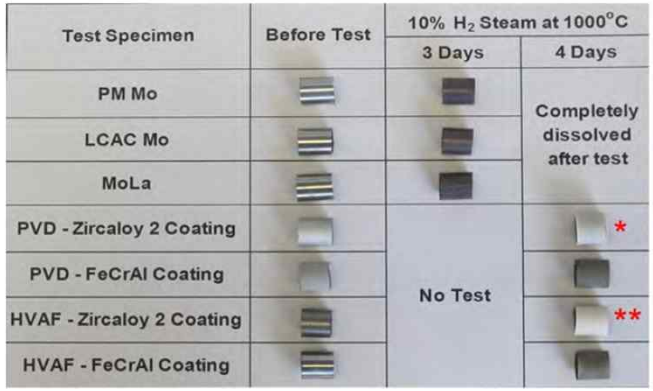

▲ Coated alloys after HT steam oxidation [3]

▲ 13Cr-5.3Al, 13Cr-6.29Al, 13Cr-7.22 FeCrAl master tube-drawn [2]

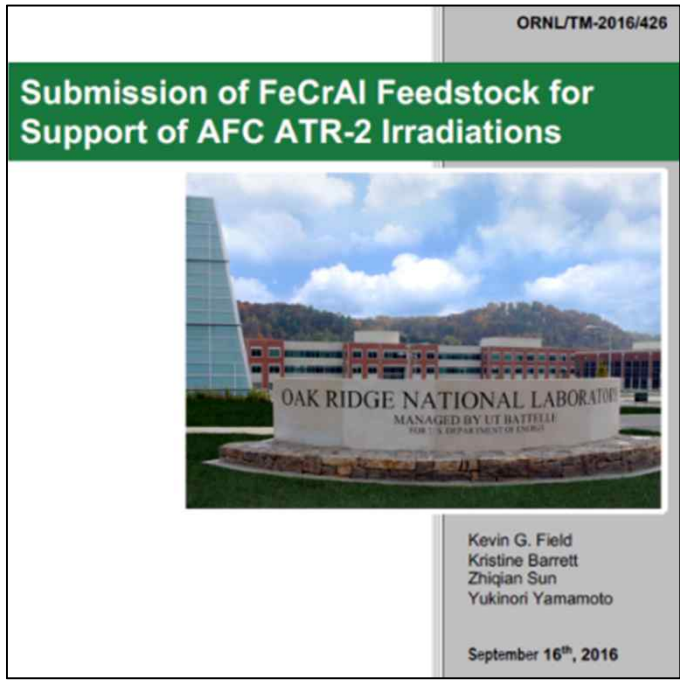

Background

S. Maloy et. al., Advs. in Nucl. Fuel and Maters. DOE Purdue WS, 2014

- Satisfactory steam oxidation resistance

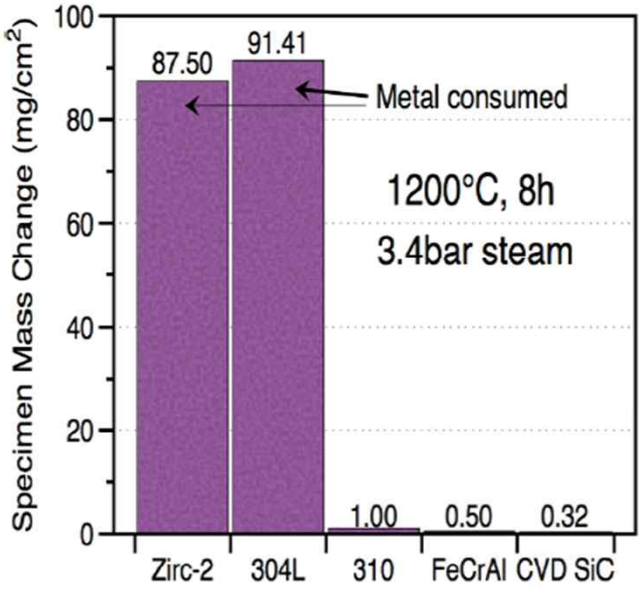

▲ **A comparison of conventional alloys and ATF candidate materials in high temp. steam oxidation**

- Some issues of candidate ATF materials
  - **Ceramic** cladding (SiC)
    - Brittle fracture in normal operation / Joining
    - Fission products retention issue
  - **Coating** on Zr-alloy (Cr/Zr)
    - Inherent Zr behaviors (balloon/burst) / Inside coating(?)
  - **Metallic** cladding (Mo, FeCrAl)
    - Poor oxidation (Mo) / Embrittlement (FeCrAl)

⇒ **Better materials for ATF?**

Development of Alumina-forming Duplex SS

Design of ADSS alloys

- Concept of ADSS alloys design

Advanced Steel (FeCrAl)

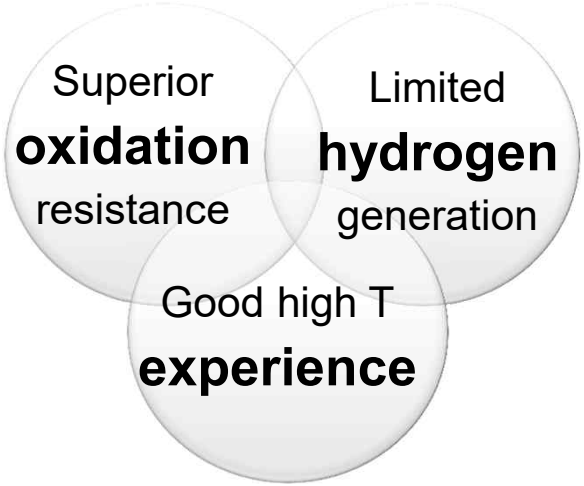

ADSS alloy

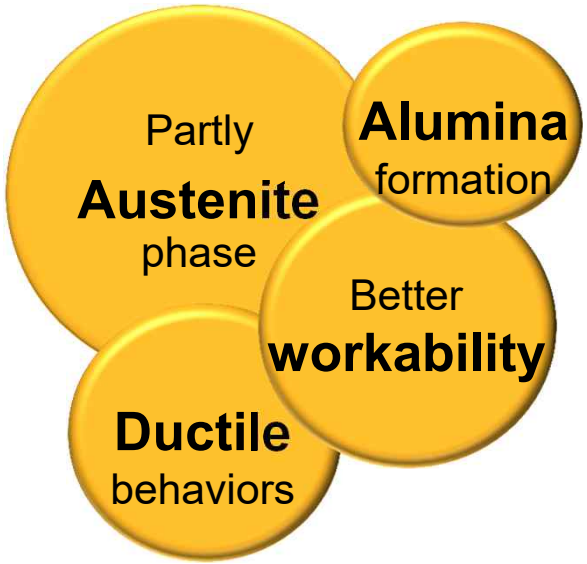

But,

Embrittlement, High temp strength?

Workability?

Design of ADSS alloys

Compositions patent (KR 10-1833404)
PCT/KR2017/010276

❑ Chemical compositions and major roles

- Ni: Austenite stabilizer, Fe-Ni spinel oxides
- Cr: Ferrite stabilizer, Fe-Cr spinel oxides
- Al: Ferrite stabilizer, alumina formation, nickel aluminide (i.e. B2-NiAl)
- Nb/Mn/C/Si: phase stability, grain size controls, SCC

Compositions (wt%)		Ni	Cr	Al	Nb	Mn	C	Si	I.D.	Structure	Note
ADSS	18Ni-16Cr-4.9Al	18.3	16.2	4.93	1.39	1.22	0.11	0.34	#B11	**Multi-plex** (Ferritic + Austenitic + B2-NiAl)	
	20Ni-16Cr-5.4Al	20.6	16.3	5.36	1.58	1.08	0.12	0.36	#B22		
	21Ni-21Cr-5.5Al	21.4	20.9	5.50	0.52	1.04	0.12	0.32	#B32		
	19Ni-16Cr-6.1Al	18.7	16.3	6.14	0.53	1.04	0.11	0.31	#B51		
Reference alloys											
FeCrAl	22Cr-5.8Al	-	21.9	5.81	-	0.16	.033	0.28	**APM**	**Ferritic**	
	21Cr-4.9Al	-	21.1	4.94	-	0.13	.037	0.34	**APMT**		Mo 2.95
ASS	19Ni-25Cr	19.1	24.7	-	-	0.87	.06	0.69	**310S**	**Austenitic**	
DSS	5Ni-22Cr	4.8	22.5	-	-	0.87	.012	0.45	**S2205**	**Duplex**	N 0.15 Mo 3.24

*ICP-AES, C/N/S - KS D 1803/1804 (RIST)

Design of ADSS alloys

H. Kim et al. J. Nucl. Mater., 507 (2018) 1

❑ Thermodynamic modeling

- Fe-(16-20)Ni-16Cr-(5.5-7.0)Al + (Nb, Mn, C, Si)
- Austenite(FCC), ferrite(BCC), nickel aluminide (B2-NiAl) co-exist
- B2-NiAl phase fraction/stability depends on Ni/Al, respectively

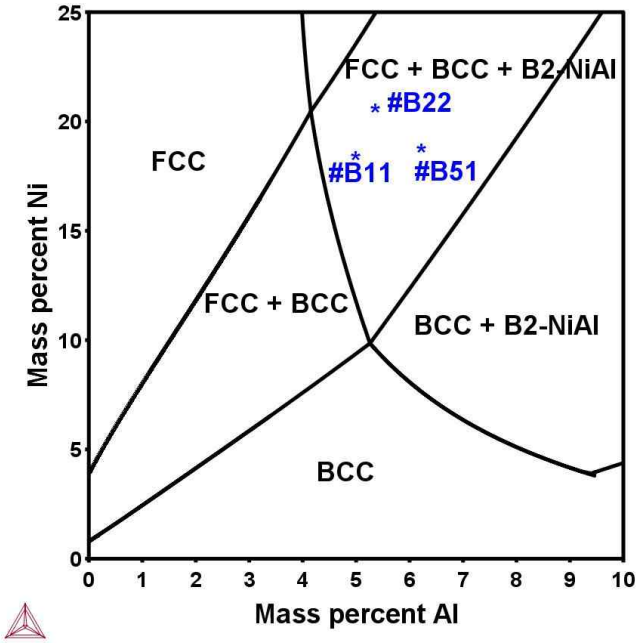

▲ Thermo-Calc phase diagram (TCFE-9 database) for Fe-16Cr-xAl-yNi system at 900°C, and the indicated target ADSS compositions.

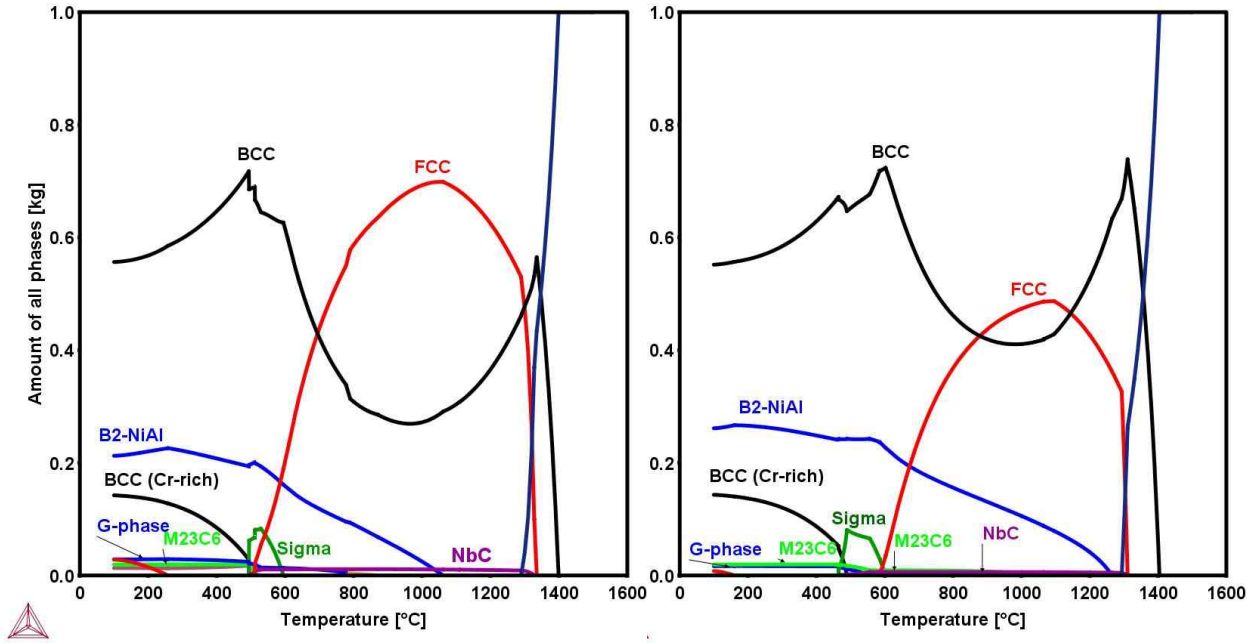

▲ Equilibrium diagram (TCFE-9 database) for predicting the phases of (left) ADSS#B11 (Fe-18Ni-16Cr-5Al), and (right) #B51 (Fe-19Ni-16Cr-6Al

Microstructure of ADSS alloys

Method/microstructure patent (KR 10-1779128)

❑ Microstructure (SEM)

- **A**ustenite(light grey), **F**errite (dark grey), **B**2-NiAl (circular black)
- Phase fraction A : F + B = 40-50 : 60-50

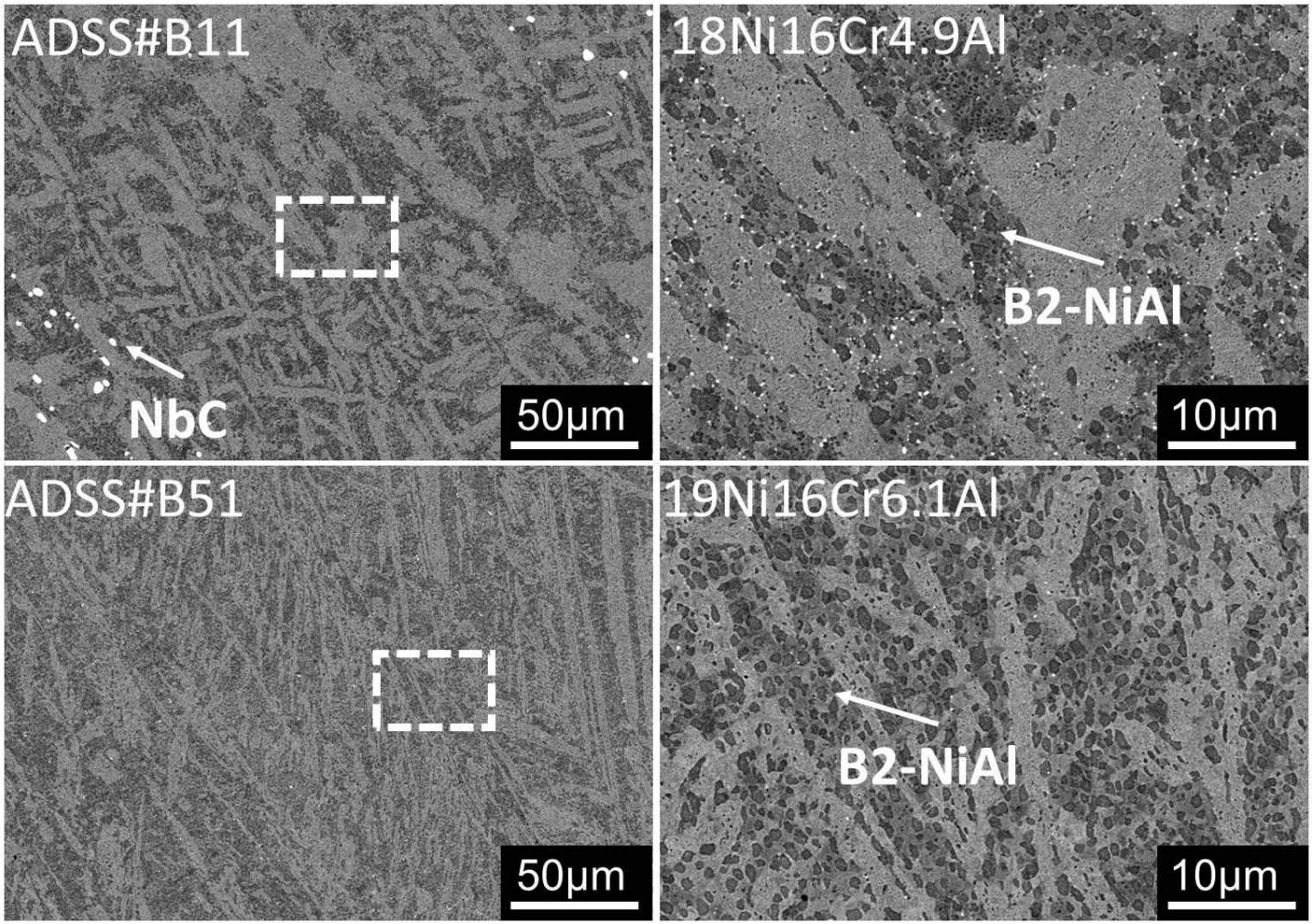

◀ SEM(BSE) images of ADSS B11 and B51 alloys in cold-rolled + final annealed (at 900°C 30 min.) condition

Microstructure of ADSS alloys

❑ Microstructure (TEM)

- Austenite-ferrite interface STEM/EDS
- Small(~50 nm)/large (~0.5 microns) size B2-NiAl phase in austenite and ferrite region, re spectively

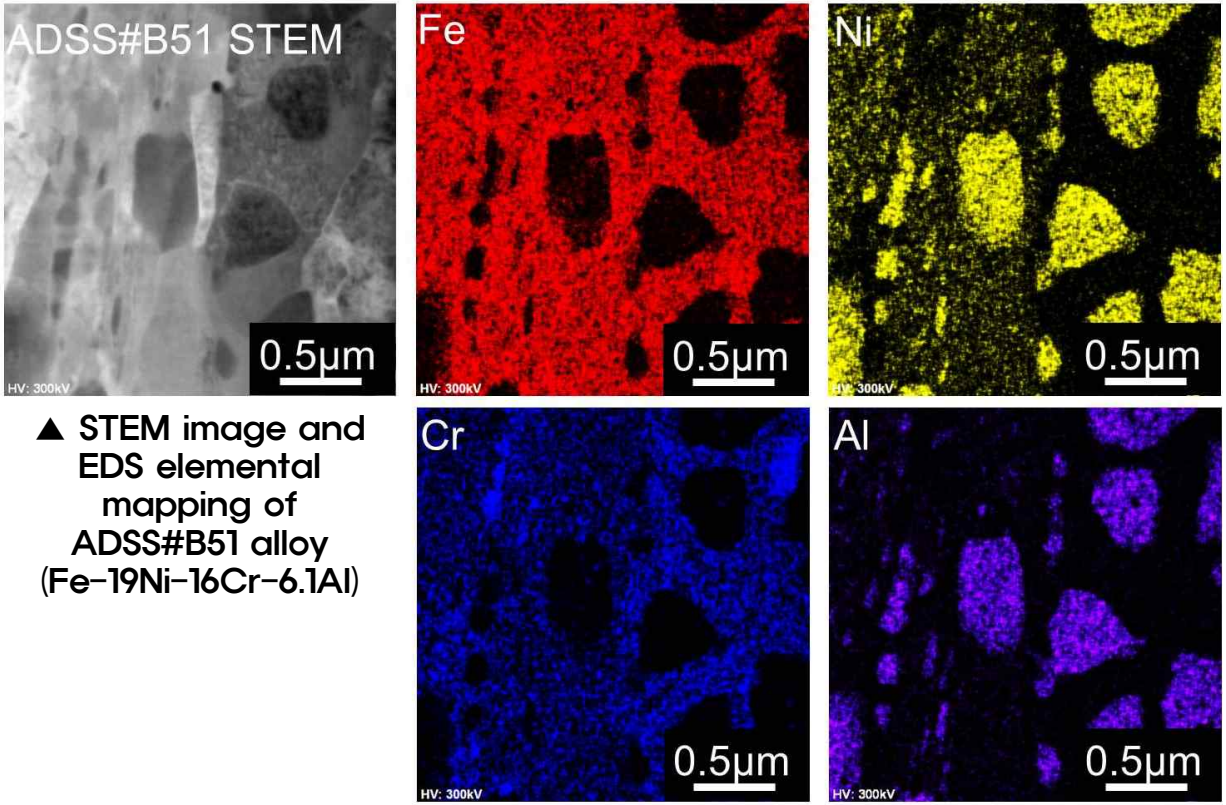

▲ STEM image and EDS elemental mapping of ADSS#B51 alloy (Fe-19Ni-16Cr-6.1Al)

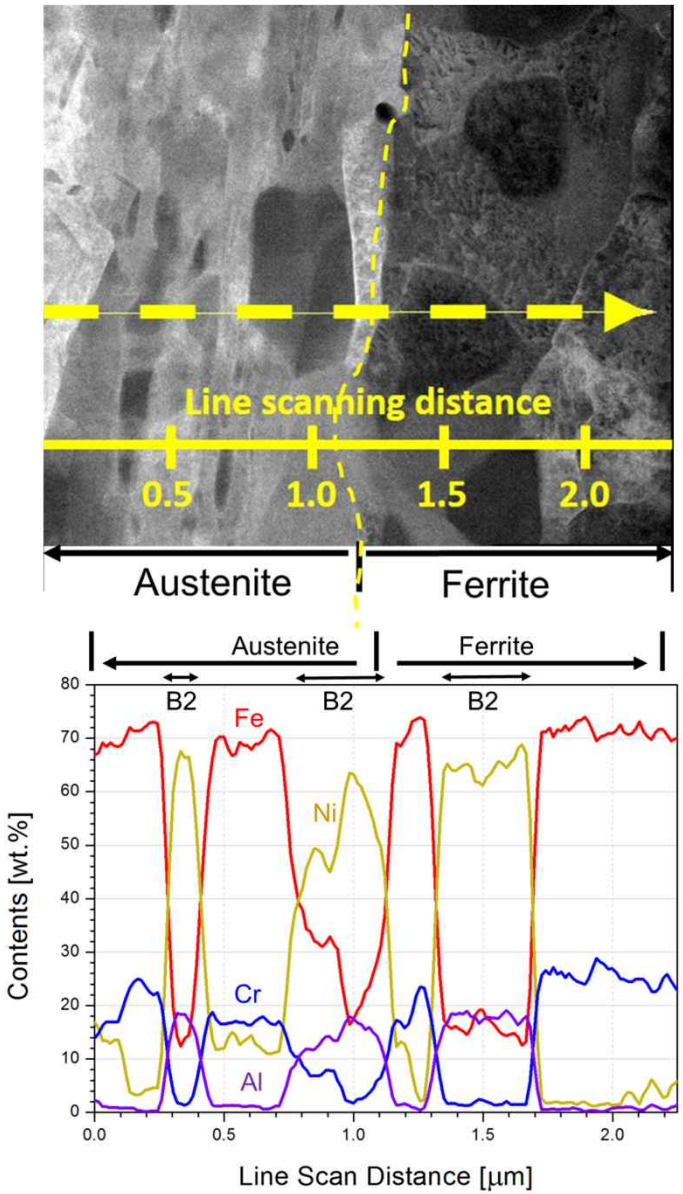

▲ Line-scan analysis results of major elements

Tensile properties of ADSS alloys

H. Kim et al. J. Nucl. Mater., 507 (2018) 1

❑ Mechanical properties

- Cold-rolled (CR) + final annealed (FA) (900°C 30min FC)

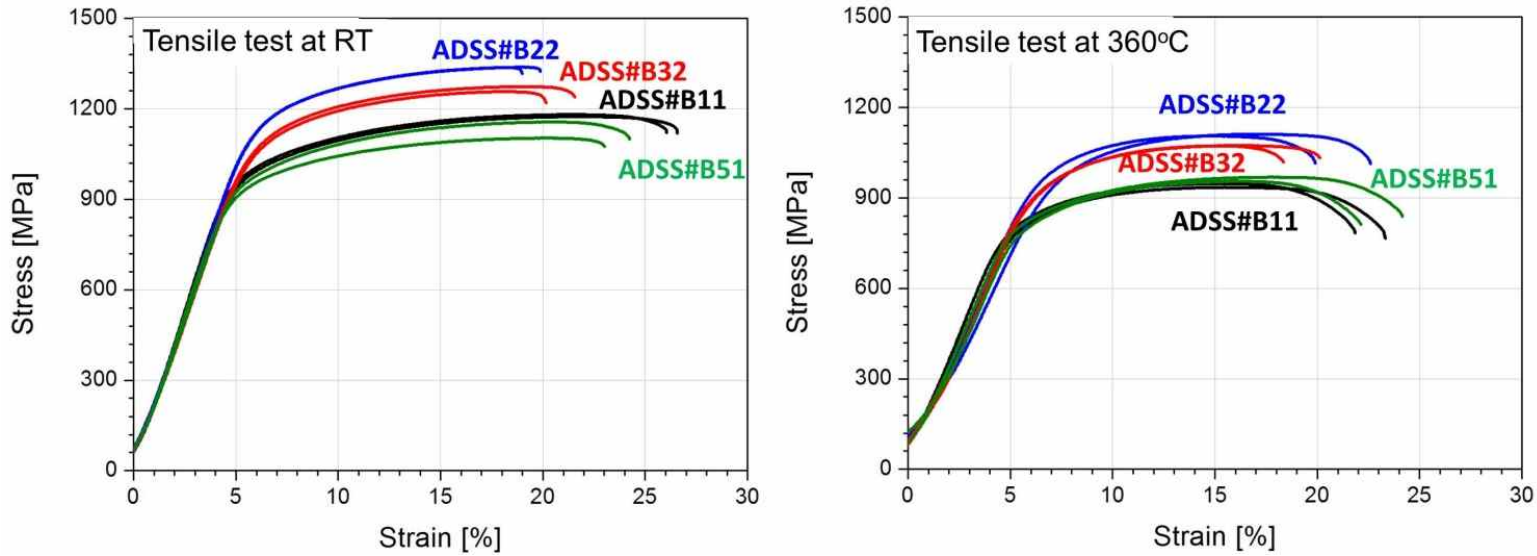

Materials (grade)	Condition	Yield strength [MPa]	Tensile strength [MPa]	Elongation [%]
Zircaloy-4	Reference materials	298 ± 9	481 ± 1	18.2 ± 0.6
APM (FeCrAl)		528 ± 19	698 ± 13	11.9 ± 0.6
310S		299 ± 8	580 ± 15	51.9 ± 1.1
DSS2205		629 ± 24	830 ± 24	34.2 ± 1.2
ADSS B11	CR+FA condition	929 ± 30	1198 ± 10	20.5 ± 0.4
ADSS B51		929 ± 30	1129 ± 38	18.5 ± 0.8

Tensile properties of ADSS alloys

❑ Mechanical properties

- YS > 800 MPa at cladding temperature (ADSS #B32)
  - For ADSS #B51, YS ~ 775 MPa
- YS/UTS decrease at 550°C
  - Rapid loss of strength for B2-NiAl phase
- ADSS alloys are much stronger than FeCrAl alloys

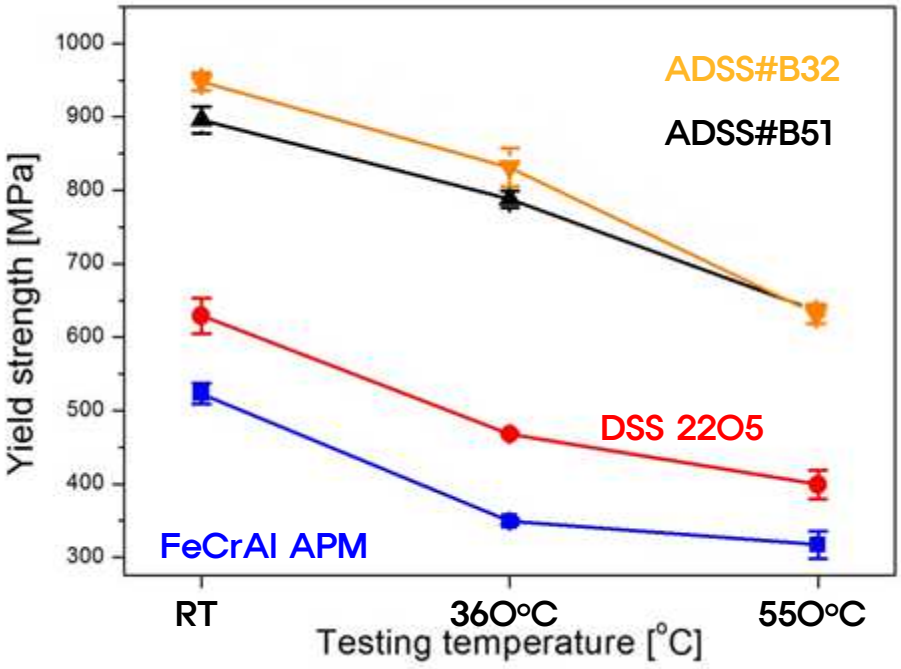

▲ YS of ADSS and reference alloys at RT, 36O°C and 55O°C

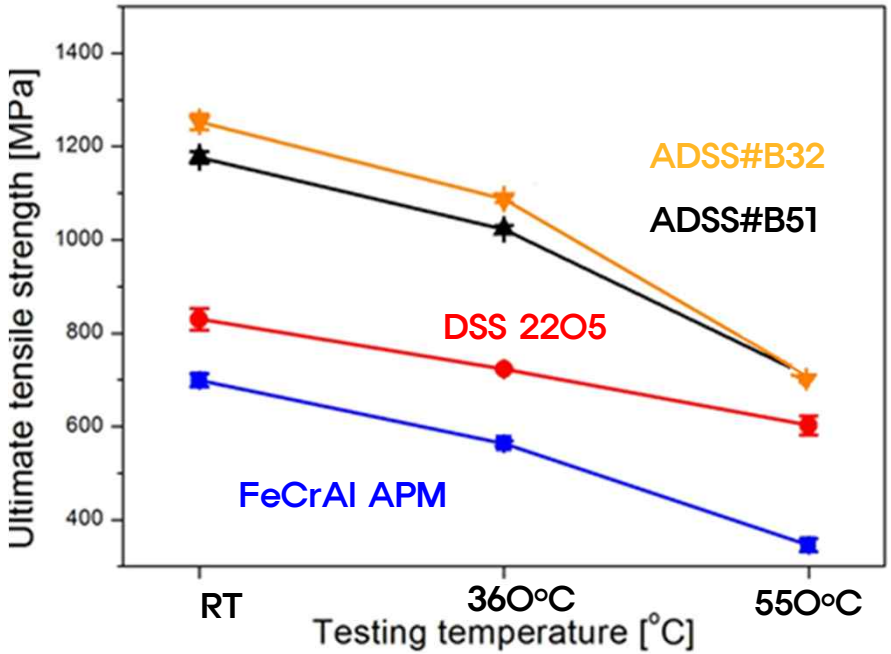

▲ UTS of ADSS and reference alloys at RT, 36O°C and 55O°C

Corrosion resistance of ADSS alloys

❑ High temperature steam oxidation

- Steam TG 1200°C 8h
- ADSS alloys showed somewhat larger weight gain, but with similar kinetics at steady-state
  - Confirmed to form protective alumina formation, comparable to FeCrAl alloys

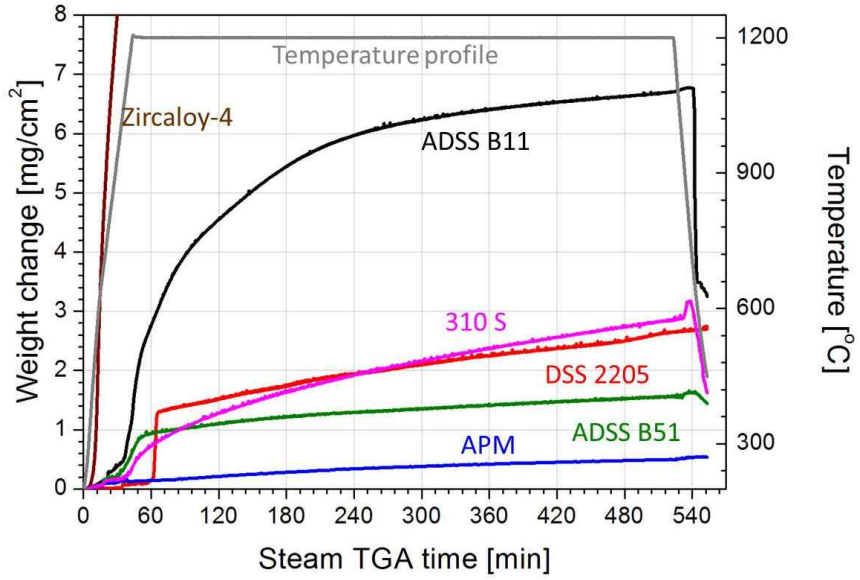

▲ Steam TG graph of ADSS and reference alloys at 1200°C for 8h

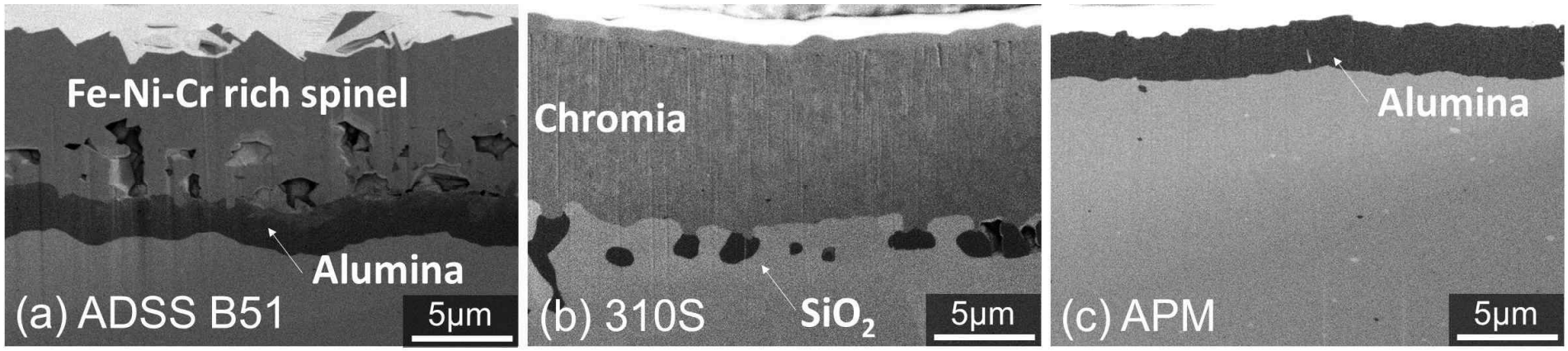

▲ Cross-sectional oxide FIB/SEM images for ADSS alloys (a) B51, (b) 310 S, and (c) APM stainless steels after exposure in steam TG at 1200 °C for 8 h.

Corrosion resistance of ADSS alloys

❑ High temperature steam oxidation

- Isothermal corrosion in steam at 800 ~ 1050°C for 24h
- Still form protective aluminum-rich oxide layer, resulting in weight gain comparable to FeCrAl alloys
- The difference with APM decrease at lower oxidation temperature

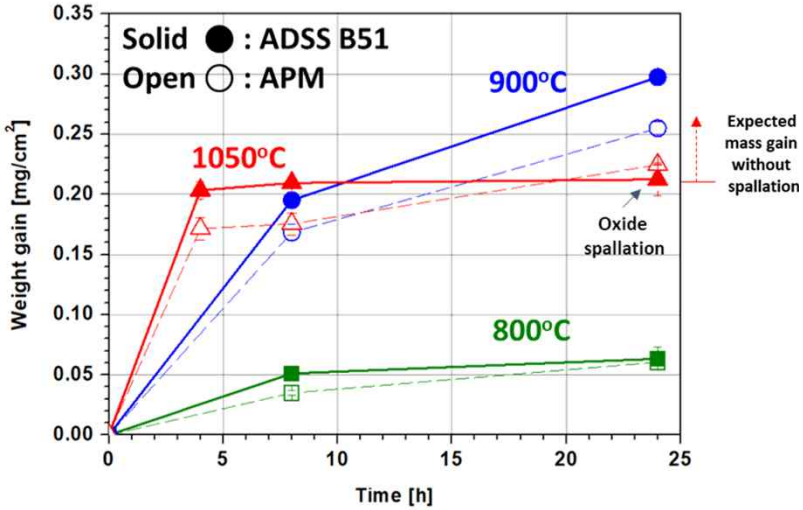

▲ Weight gain results of ADSS #B51 and APM at 800°C ~ 1050°C for 24h

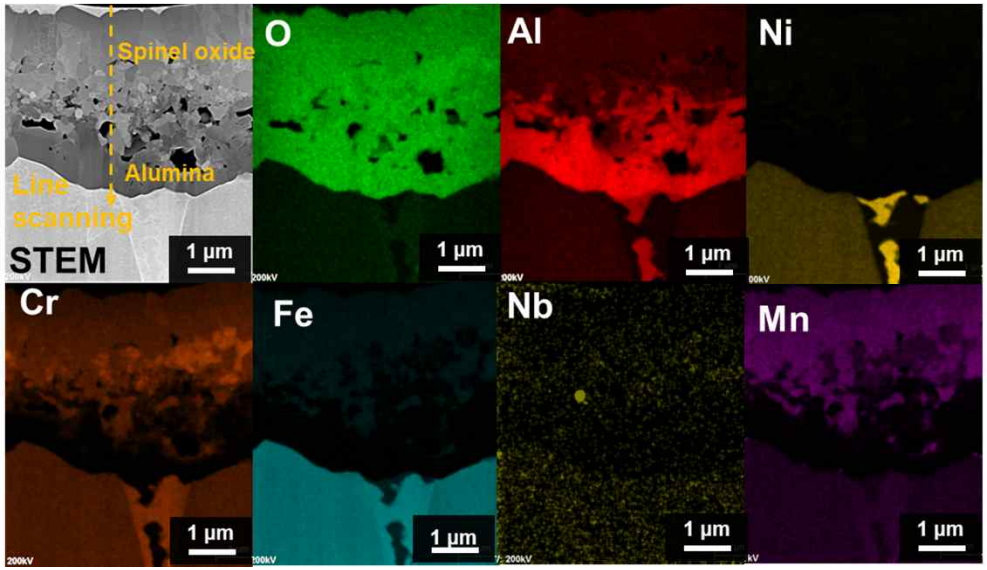

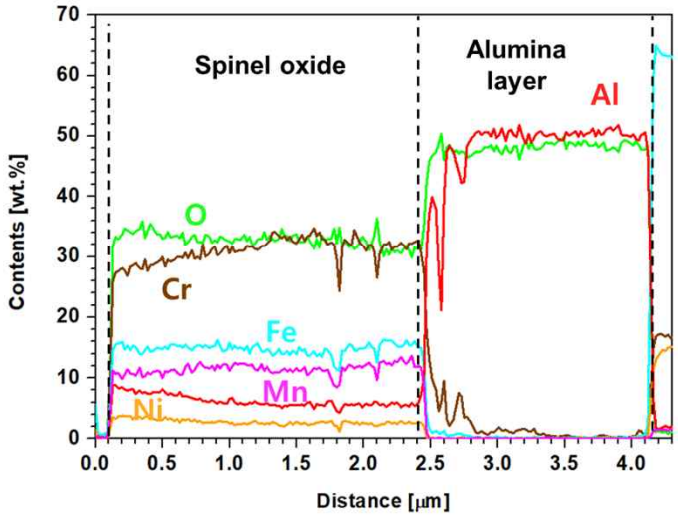

▲ STEM/EDS elemental mapping results and line scanning of ADSS#B51 after 1050°C 24h steam exposure

Corrosion resistance of ADSS alloys

H. Kim et al. J. Nucl. Mater., 507 (2018) 1

❑ PWR corrosion

- Spinel oxides + continuous chromia
- ADSS alloys showed excellent corrosion resistance comparable to 310S SS

Table 6
Mass gain and oxide thickness after 30 days corrosion in the simulated PWR environment.

Materials	Mass gain [mg·dm^{-2}]	Oxide thickness [μm]
ADSS alloys	0.62 ± 0.30	0.05–0.15
APM	-0.33 ± 0.06	–
310 S	Negligible[a]	<0.01
Zircaloy-4	20–30	1.3–2.0[b]

[a] Mass gain less than 0.03 mg dm^{-2}.
[b] Values estimated from the longer-term data.

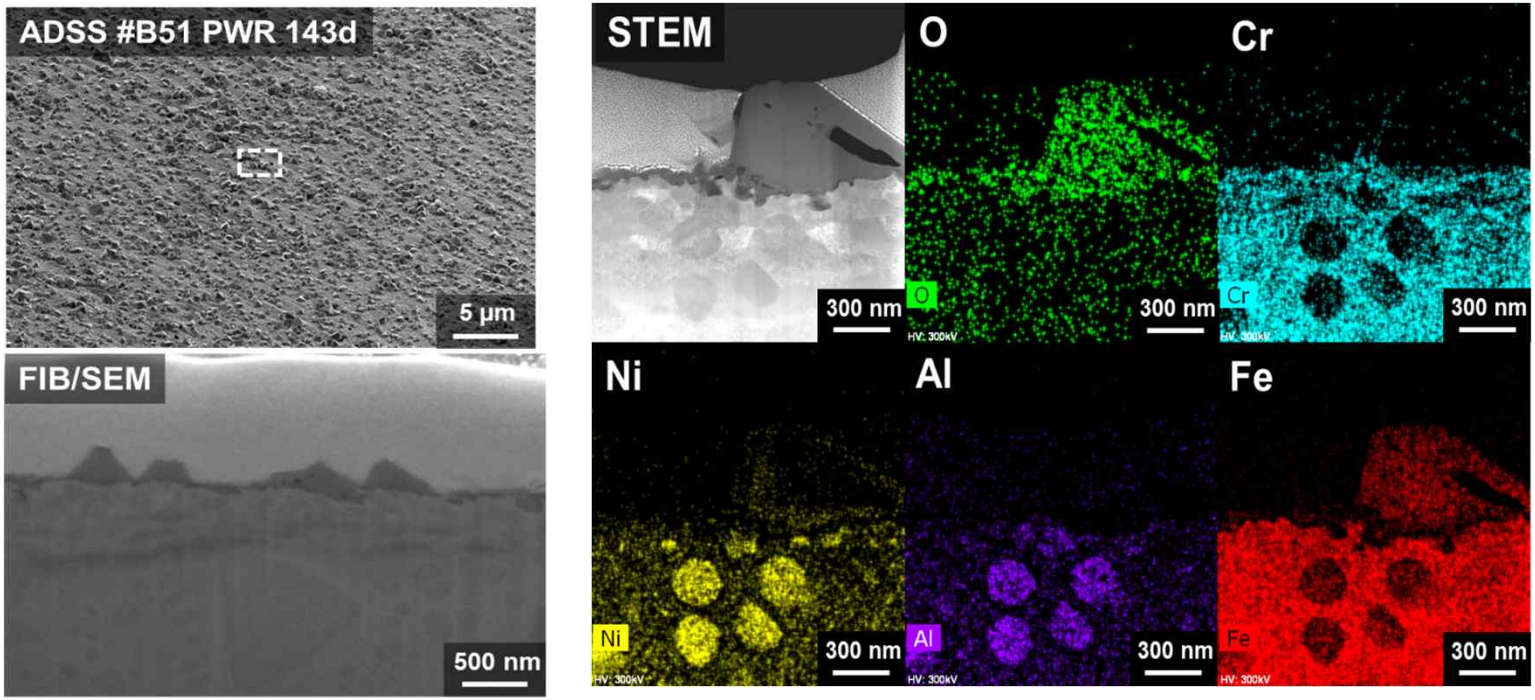

▲ FIB/SEM images and STEM/EDS mapping results of ADSS #B51 after PWR exposure for 143days

Corrosion resistance of ADSS alloys

❑ High temperature oxidation after PWR-exposure

- PWR exposure for 143 days → 1200°C 8h steam exposure
- 30% reduced weight gain after PWR-exposure than virgin condition
  - Similar steady-state oxidation kinetic but, difference initial weigh changes
  - Spinel oxides(formed during PWR exposure)
    → suppress the high temperature oxidation at initial transient stage

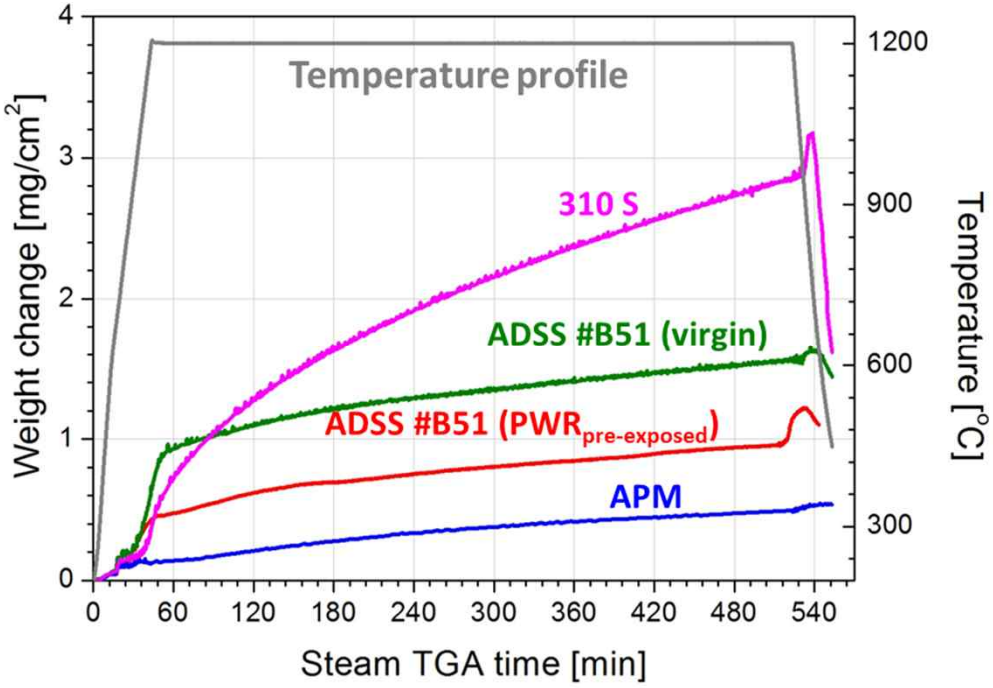

▲ Steam TG graph of virgin and PWR pre-exposed ADSS #B51 with reference alloys at 1200°C for 8h

Thermal aging embrittlement

❑ 425 °C thermal aging for upto 1khr

- All Fe-based alloys, embrittlement (YS↑, elongation ↓)
- The degree of thermal aging, ADSS << AF
  - Due to austenite phase in ADSS
- Austenite phase : ADSS #B11 > ADSS #B32
- Degree of thermal aging : ADSS #B11 < ADSS #B32

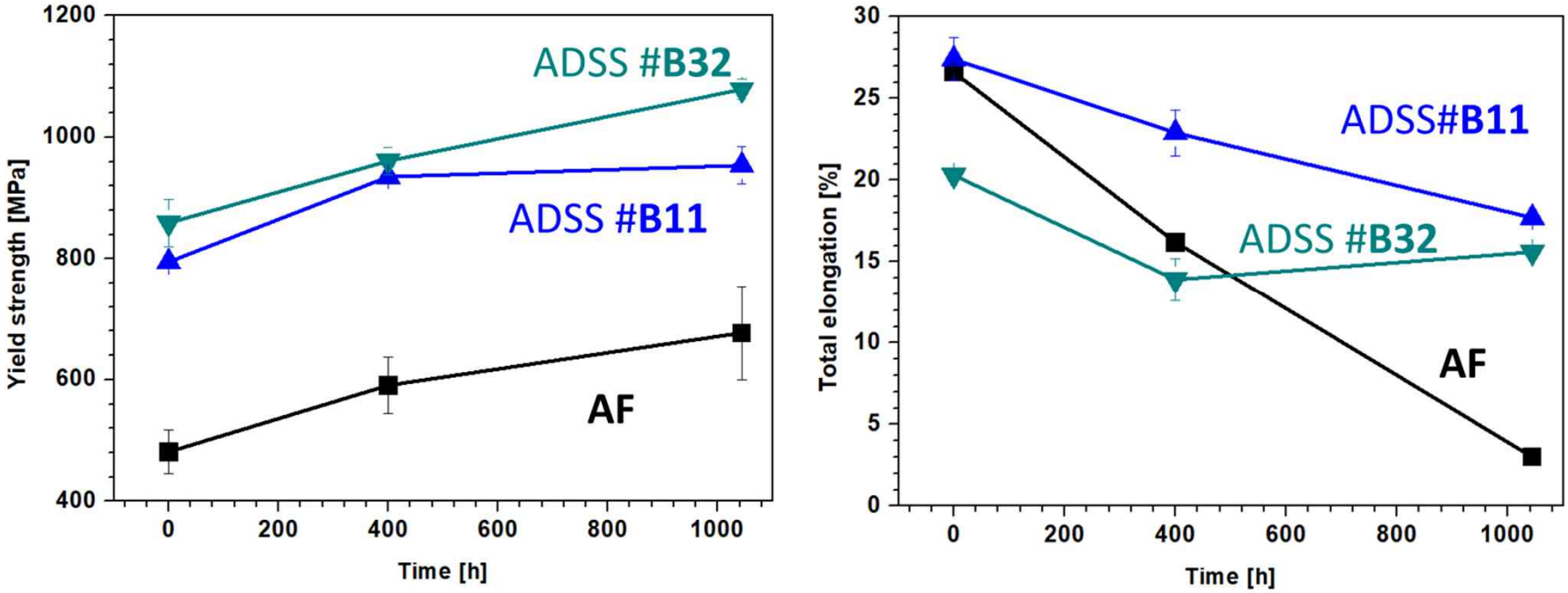

▲ YS and total elongation of ADSS alloys and AF after thermal aging at 425 °C for up to 1khr

Neutronics Analysis of ADSS Alloys as Fuel Cladding

Neutronics penalty on fuel cycle

❑ Neutron penalty of ADSS cladding

- High thermal neutron absorption c-x of transition elements (Ni, Cr, Fe)
  - Loss of excess reactivity → short refueling period
- Simplified assembly calculation was performed for PWR 16x16 PLUS7 fuel assembly using KARMA code in KEPCO NF
- Negligible change in effective full power day (EFPD), if
  - Increase in nominal U^{235} Enrichment: 4.65 → 4.95 %
  - Reduce clad thickness: 0.57 mm => 0.35 mm (with larger UO_2 pellet)

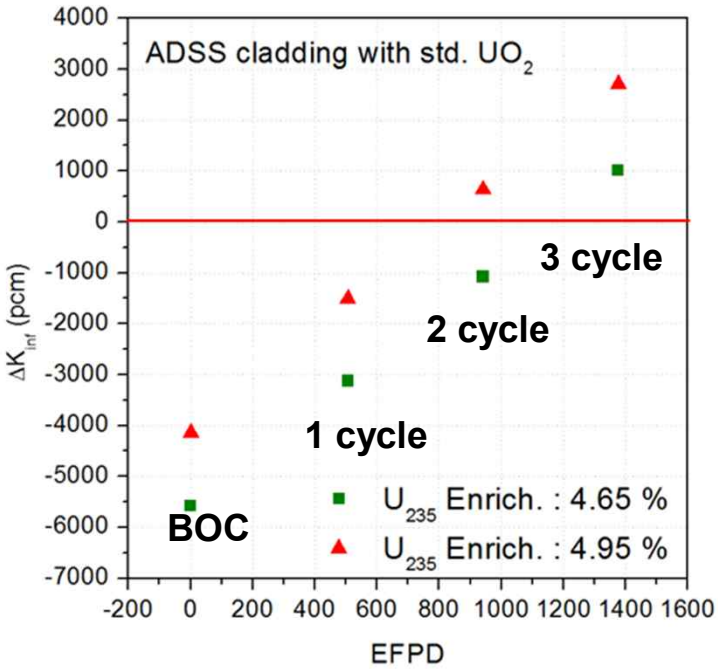

▲ Change in reactivity as function of EFPD for ADSS/UO_2 system with different enrichments

◀ **Fuel rod geometries of current Zr/UO_2 system and ADSS/UO_2 system**

Uranium enrichment [wt.%]	Fuel cycle 1	Fuel cycle 2	Fuel cycle 3
4.65	-104 days	-36 days	34 days
4.95	-50 days	21 days	90 days

▲ Changes in EFPD of ADSS cladding as an function of UO_2 enrichment

Helium production in ADSS cladding

❑ He production of ADSS cladding

- For neutronics analysis, SERPENT2 (Monte Carlo code) was used
- Consider 17x17 ACE7 WH design
- Analysis conditions

$$^{58}Ni(n,\gamma) \rightarrow {}^{59}Ni(n,\alpha) \rightarrow {}^{56}Fe$$

Case	Material	Pellet diameter (cm)	Cladding thickness (cm)
1 (Ref)	Zircaloy – 4	0.81916	0.05817
2	ADSS #B11	0.81916	0.05817
3	ADSS #B11	0.87370	0.3
4	ADSS #B22	0.81916	0.05817
5	ADSS #B22	0.87370	0.3
6	ADSS #B32	0.81916	0.05817
7	ADSS #B32	0.87370	0.3
8	ADSS #B51	0.81916	0.05817
9	ADSS #B51	0.87370	0.3

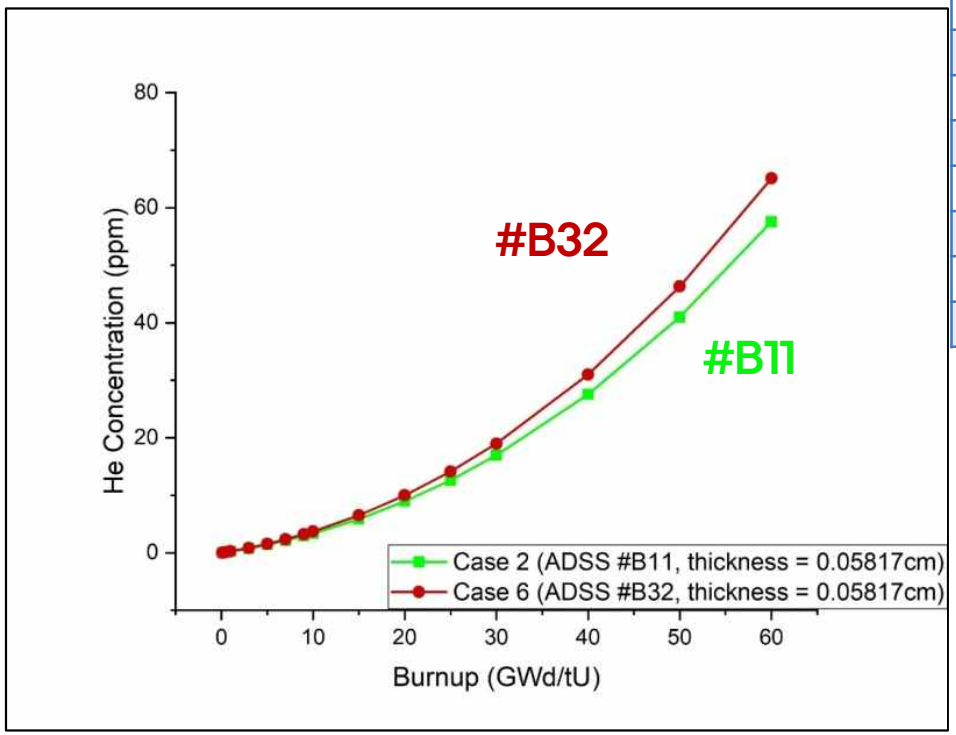

▲ Helium production in ADSS cladding

- Ni contents :: #B11(18.3wt.%)/#B32 (21.4wt.%)
- He production ↑ by increasing Ni contents

Decay Heat from ADSS Cladding

❑ Decay heat from of ADSS cladding

- ORIGEN ARP code was used
- Source of decay heat :
  $^{95}Nb/^{95}Zr$ for Zr-alloys
  $^{58}Co/^{60}Co/^{54}Mn$ for ADSS alloys
- Same thickness with Zr-alloys
  - Slightly higher decay heat
- Reduced thickness (0.3 mm)
  - At BOC, decay heat less than Zr-alloys
  - The fraction of decay heat < 0.4%

Case	Material	Pellet diameter (cm)	Cladding thickness (cm)
1 (Ref)	Zircaloy - 4	0.81916	0.05817
2	ADSS #B11	0.81916	0.05817
3	ADSS #B11	0.87370	0.3
4	ADSS #B22	0.81916	0.05817
5	ADSS #B22	0.87370	0.3
6	ADSS #B32	0.81916	0.05817
7	ADSS #B32	0.87370	0.3
8	ADSS #B51	0.81916	0.05817
9	ADSS #B51	0.87370	0.3

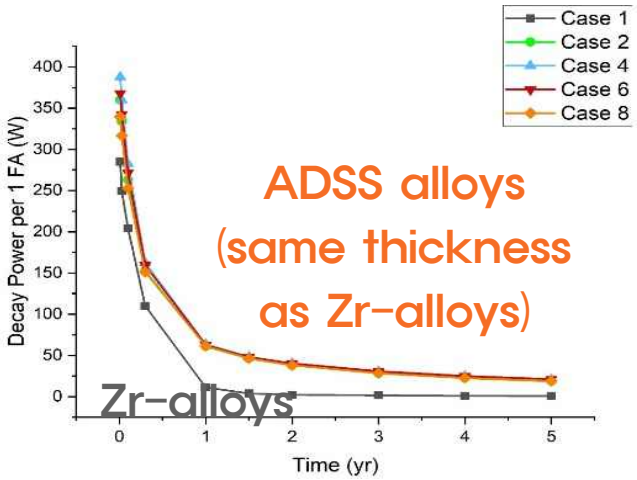

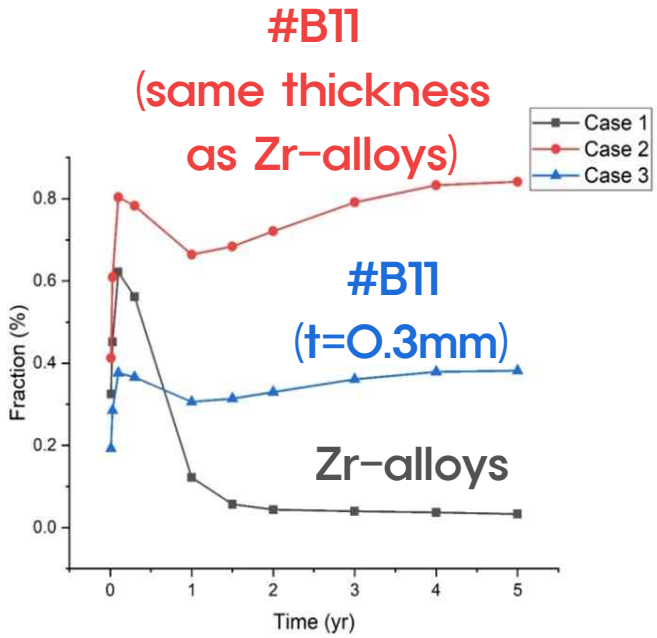

▲ **Decay power in the claddings from assembly calculation**
(left) decay power per assembly and (right) fraction of decay heat from cladding to total decay heat

Fabrication of thin ADSS cladding tube

❑ Fabrication of thin tube

- Cladding geometry: OD/TH/L (8 mm / 0.30mm / 1.6m)
- Master-bar production
  - Ingot → forging + hot-rolling → heat treatment(HT)
  - Practical approaches suitable for the production line
- Tube fabrication: Gun-drilling – pilgering – final HT

▲ **the process of master bar production and fabricated thin ADSS tubs by pilgering**

Fabrication of thin ADSS cladding tube

❑ Fabrication of thin tube

- Pilgering results
  - Finished product:
    OD 8 mm x T 0.3 mm x L 1600 mm
- Similar microstructure (austenite + ferrite + B2-NiAl) and mechanical properties (UTS~1GPa) with cold-rolled plates

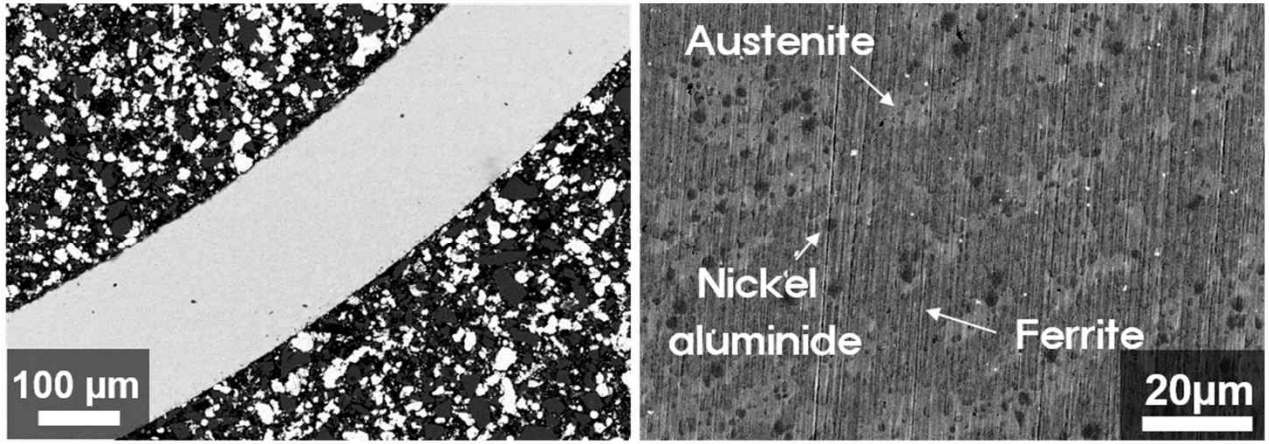

▲ microstructure of ADSS thin tube

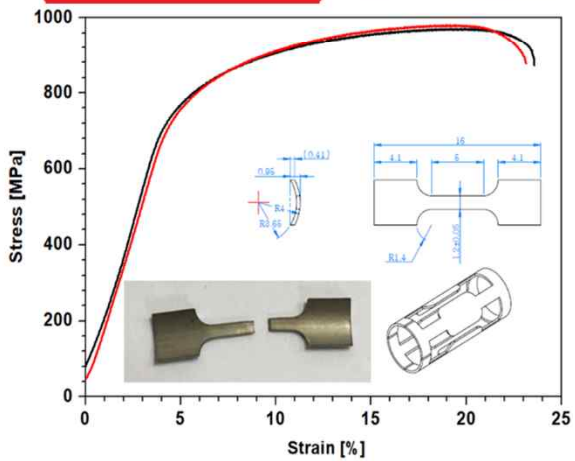

▲ Mini-tensile results of thin tube

Summary

Summary

- **Development of alumina-forming duplex stainless steels (ADSS)**
  - Nominal composition of Fe-(16-20)Ni-16Cr-(5.5-7.0)Al + minor elements
    - Austenite(FCC), ferrite(BCC), nickel aluminide (B2-NiAl) co-exist
  - Protective oxide layers in both normal and accident conditions
    - Chromia in PWR environment / Alumina in Accident environment
  - High strength (UTS ~ 1GPa) and ductility (UE ~ 15 %)
    - Structural integrity can be obtained with very thin (~ 0. 35 mm) tube
  - Less thermal embrittlement than ferritic FeCrAl due to austenite phase

- **Neutronics penalty could be accommodated**
  - Large thermal neutron c-x could be accommodated with thinner cladding (~ 0.35 mm) and/or increase in fuel enrichment (4.65% to 4.95%).
  - Helium production was estimated about 60 appm for ADSS alloys.
  - The decay power from the transmutation of alloying elements was less than 0.4% of total decay power from the fuel, which was considered negligible.

- **Fabrication of thin ADSS cladding tube**
  - Initial fabrication of thin tube (0.3 mm thickness and 1.6m long) was successful with pilgering

KAIST

NQe Department of Nuclear & Quantum Engineering

NU_Html Nuclear & High Temperature Materials Laboratory

KEPCO NF

Energy for Earth !!

Thank you!